

# Spatiotemporal changes in the size and shape of heat waves over North America

David Keellings 1 Description • Erin Bunting 2 • Johanna Engström 2

Received: 31 July 2017 / Accepted: 5 January 2018 / Published online: 23 January 2018 © Springer Science+Business Media B.V., part of Springer Nature 2018

Abstract Heat waves are occurring more frequently across the globe and are likely to increase in intensity and duration under climate change. Much work has already been completed on attributing causes of observed heat waves and on modeling their future occurrence, but such efforts are often lacking in exploration of spatial relationships. Based on principles of landscape ecology, we utilized fragmentation metrics to examine the spatiotemporal changes in heat wave shape and occurrence across North America. This methodological approach enables us to examine area, shape, perimeter, and other key metrics. The application of these shape metrics to high-resolution historical (1950–2013) climate data reveals that the total number and spatial extent of heat waves are increasing over the continent, but at an individual heat wave patch level, they are becoming significantly smaller in extent and more complex in shape, indicating that heat waves have become a more widespread and fragmented phenomena.

### 1 Introduction

Heat waves are reportedly occurring more frequently across much of the globe, and under a warming climate, they are expected to increase in frequency, intensity, and duration (Diffenbaugh and Ashfaq 2010; Barriopedro et al. 2011; Coumou and Rahmstorf 2012; IPCC 2014). Heat waves are extreme meteorological events that can have pronounced impacts on health, air quality, and vegetation (Easterling et al. 2000; Ciais et al. 2005; Vautard et al. 2005; Centers for Disease Control and Prevention (CDC) 2006; Comrie 2007; Ebi 2008). The occurrence of heat waves and their detrimental health impacts are evident in recent events,

**Electronic supplementary material** The online version of this article (https://doi.org/10.1007/s10584-018-2140-3) contains supplementary material, which is available to authorized users.

□ David Keellings djkeellings@ua.edu



Department of Geography, University of Alabama, Tuscaloosa, AL 35487, USA

Department of Geography, University of Florida, Gainesville, FL, USA

such as those in 2003 (Central Europe), 2010 (Russia), and 2012 (USA) as high temperatures exacerbate pre-existing medical conditions and cause overall mortality rates to increase (Kunst et al. 1993; Curriero et al. 2002; Hajat et al. 2002; Comrie 2007; Ebi 2008). A recent study found that almost half of the world's population would likely be annually exposed to lethal heat wave events by 2100 (Mora et al. 2017). Additionally, changes in heat wave pattern, intensity, and duration impact the soil water balance across terrestrial ecosystems resulting in cascading effects to flora, fauna, ecosystem services, and overall landscape production (Toomey et al. 2011). Heat waves have direct and indirect effects on ecosystems and agricultural products as a result of higher water loss through evapotranspiration (Zaitchik et al. 2006; Schlenker and Roberts 2009), and extreme heat is often accompanied by increased electricity consumption, spikes in air pollution, and wildfires (Bernard et al. 2001; Vautard et al. 2005; Zamuda et al. 2013).

Heat waves can be defined as a sequence of days/nights with maximum/minimum temperature above a certain high percentile threshold, which have variously been described as being between the 90th and 99th percentiles of the daily maximum temperature distribution (Anderson and Bell 2009; Hajat et al. 2006; Keellings and Waylen 2014a; Keellings and Waylen 2014b; Mazdiyasni and AghaKouchak 2015; Meehl and Tebaldi 2004; Peng et al. 2011; Photiadou et al. 2014). In this study, the 95th percentile of the entire distribution of daily maximum temperature is adopted as a common threshold to identify an extremely hot day. These threshold levels are calculated separately for each grid cell from the entire temperature record (1950–2013) at each grid cell. Heat waves can also be defined by their duration in terms of how many consecutive days of above threshold temperatures occur (Tan et al. 2007). In this study, a duration criterion of at least 3, 5, or 7 days of consecutive above threshold days is set. However, the methods developed here are equally suitable for use with other thresholds, defined in either the frequency (percentiles) or magnitude (temperature) domains, for specific applications. Past studies of heat waves over North America have found widespread positive trends in the frequency of heat waves during the latter half of the twentieth century, with the largest trends observed in urban locations (Gaffen and Ross 1998; DeGaetano and Allen 2002). A recent study examined the areal extent of heat waves finding an upward trend in the percent of the Continental United States (percentage of total land area) in concurrent drought and heat wave (Mazdiyasni and AghaKouchak 2015). A so-called 'warming hole' or negative trend in the upper tail of daily maximum temperatures was observed in the southeast US during 1951–1975 and then in the central US from 1976 to 2000 (Pan et al. 2013). These warming holes have been linked to regional changes in the hydrological cycle brought about, at least partly, by the effect of aerosol emissions on clouds (Leibensperger et al. 2012; Yu et al. 2014) and land surface interactions (Kunkel et al. 2006). Large-scale atmospheric oscillations, including the Pacific Decadal Oscillation (PDO) and the Atlantic Multi-decadal Oscillation (AMO), have also been linked to the appearance of these warming holes (Robinson et al. 2002; Kunkel et al. 2006; Wang et al. 2009; Meehl et al. 2012; Kumar et al. 2013). The changing phases of the PDO and AMO are thought to be the cause of the relocation of the warming hole from the southeast to central US and the appearance of a more recent cooling trend in the northwest US (Pan et al. 2013; Meehl et al. 2015). However, cooling trends or warming holes are thought to be absent in recent decades across all regions of North America (Grose et al. 2017).

Most analyses of climate and weather extremes, such as heat waves, typically tend to focus on identifying trends, attributing causes of observed events, and on modeling their future occurrence using methods from climatology such as time-series analysis, dynamical modeling, synoptic classification, and extreme value analysis. For example, past studies of heat waves



have generally focused on identifying trends in heat wave characteristics such as frequency, magnitude, or duration (Coumou and Robinson 2013; Perkins et al. 2013; Keellings and Waylen 2014a). Much of this work focuses on changing temporal relationships within observations or simulations, but it is often lacking in exploration of spatial relationships within the dataset as conclusions are often drawn across the entire extent of the dataset or at individual regions, points, or grid cells within it. While heat waves are known to have become ever more frequent and intense, little is known about changes in the spatiotemporal patterns of heat waves across the globe. Such information is currently lacking, but is critical to gaining further understanding of the influence landscape processes, such as land cover change, have on extreme heat and giving insight into how climate change may be manifesting itself on the distribution of heat waves across the land surface. The lack of existing research on changes in important heat wave indicators such as areal extent has been highlighted by other researchers (Chen and Li 2017). Spatiotemporal patterns of extreme heat are also important in planning for future public health impacts and response during heat wave events (Hattis et al. 2012).

In this study, we examine a high-resolution historical temperature dataset using combined methodology from the fields of Climatology and Landscape Ecology to identify changes in both the temporal and spatial characteristics of heat waves across North America from 1950 to 2013. We conceptualize heat waves as patches of heat on the landscape and evaluate changes in the number, area or size, and shape of heat wave patches throughout the record. Through this combined methodology, we demonstrate how simple shape metrics may be used to assess trends in the spatial extent (size of areas impacted during a heat wave) and fragmentation (spottiness of areas impacted during a heat waves across North America.

### 2 Data

The temperature dataset is model-derived from observed data developed for the North American Land Data Assimilation System Variable Infiltration Capacity simulations over North America (http://www.colorado.edu/lab/livneh/data) (Maurer et al. 2002; Livneh et al. 2015). These daily data have a spatial resolution of 1/16° for the period 1950–2013. The dataset is compiled from over 10,000 National Oceanic and Atmospheric Administration (NOAA) Cooperative Observer Network (COOP) stations, gridded using a synergraphic mapping system (SYMAP) algorithm (Shepard 1984; Widmann and Bretherton 2000), and then interpolated using an asymmetric spline (Maurer et al. 2002).

The regions used to subset the North American data were constructed to be identical to the regions used by the North American Regional Climate Change Assessment Program (NARCCAP) (Mearns et al. 2012). The NARCCAP regions are essentially based on ecoregions that have similar variations in temperature and precipitation and can therefore be considered to have a similar climatology.

### 3 Methods

To delineate heat wave areas, each grid cell exceeding its 95th percentile of the entire (1950–2013) summertime (June–September) daily maximum temperature is identified. We have repeated the analysis using the 85th percentile threshold with those results shown in Supplementary Materials. Thus, a binary image of heat waves, above each percentile threshold, is



created for each summertime day; then, at each grid cell, the total summer heat wave days are summed to create a new single image for the entire summertime. A count of 3, 5, and 7 consecutive summer heat wave days is also summed for each grid cell. For example, a 5-day heat wave above the 95th percentile threshold is defined as 5 consecutive days of maximum temperature exceeding the 95th percentile of the entire summertime climatology at that grid cell. Events are considered to be independent if separated by at least 4 days of below threshold temperatures; otherwise, data of consecutive events are amalgamated (Keellings and Waylen 2014b). Independence criterion was set in this manner to account for the possible public health impact of having fewer than four relief days between events (Curriero et al. 2002). The total summertime count values in each grid cell of the image are then reclassified based on their relative position in the cumulative distribution function (CDF) of all counts greater than 0, the higher the count the less probable its occurrence and the higher the classification (Table S1). In this manner, we can create a single surface of reclassified counts for each summer. For example, the summer raster layers (one layer for each of 64 summers, 1950-2013) for events above the 95th percentile lasting 7 days in duration will be made up of only the class values of 1, 2, or 3 and no data for cells where the threshold was not exceeded or duration not met (Table S1). More than one heat wave may occur during a single summer, and by using this approach, we can account for multiple heat wave events in any given grid cell. The reclassification of each grid cell based on number of events and the empirical CDF gives an indication of heat wave event frequency in each cell as the higher the classification, the greater the prevalence of heat wave during that summertime. For example, a grid cell with a 5-day event classification of 2 signifies that two 5-day events occurred in that grid cell during a single summertime and falls between the 0.92 and 0.99 cumulative probability of all 5-day event counts (Table \$1).

Fragmentation metrics were calculated in R, using the SDMTools (Species Distribution Modeling Tools) and raster packages, for the spatial and temporal span of the data set. Such metrics are traditionally computed based on land cover classifications. Here, the classification of each grid cell is determined by the CDF-based reclassification of counts of heat wave events occurring in each grid cell. In this instance, the reclassified heat wave rasters were utilized as "classes," meaning that we could determine the changes in shape and size of multiple heat waves across North America based on summertime frequency, duration, and threshold exceedance. In R, the clump function was used to identify each individual heat wave patch by class across the landscape with adjacent cells sharing at least a corner (Queen's case). The output of this analysis included individual patch area (square meters) and patch perimeter (meters). The perimeter/area ratio of each patch was calculated from this output. From these individual patch metrics, the following aggregated statistics were then calculated: mean perimeter/area ratio, mean patch area, total patch area, and patch count. Each of these metrics was produced for the entirety of North America and within each ecoregion.

Changes in each of the heat wave spatial metrics through the record are investigated here to give a quantification of how heat waves may be evolving spatially. Each metric indicates different spatial aspects such as extent and fragmentation. Patch area and patch count separately show the extent and frequency of heat waves on the landscape and when combined give an indication of heat wave fragmentation. If, for example, individual patch area declines are accompanied by increased patch count then fragmentation must increase, as there are more, smaller patches. It is also of interest to examine the spatial configuration of heat wave patches beyond the simple measure of area. We explore heat wave patches further by examining heat wave patch complexity, which refers to the actual geometry or shape of patches. Shape is



difficult to capture given the high variability that may be possible in the configuration of patches, but a simple measure of shape is the ratio of perimeter to area. Higher values of perimeter/area ratio equate to greater shape complexity or further departure from simple Euclidean geometry (Mcgarigal 2015). For an illustrated description of these metrics, please see Fig. S7.

The two-sample Kolmogorov-Smirnov (KS) test assesses differences between CDFs based on distance between empirical distribution functions. This is a non-parametric test with the null hypothesis that the two distribution functions are drawn from the same continuous distribution (Stephens 1970). A bootstrapped version of the KS test that is insensitive to ties with discrete data is implemented here (Sekhon 2011). Here, we use the two-sample KS test with bootstrapping to determine whether data from the first half of the record (1950–1981) and the second half of the record (1982–2013) come from the same distribution at the 0.05 significance level (95% confidence). The use of the KS test in this manner allows us to identify long-term trends or shifts in the distribution of individual patch metrics (Mazdiyasni and AghaKouchak 2015). The Mann-Kendall (MK) trend test (Mann 1945; Kendall 1955) assesses the presence of a statistically significant (0.05 significance level) trend in the time series of total patch area and patch count through the entire record (1950–2013). The non-parametric MK trend estimator is commonly used in climatology to assess trends in time series, and here, we apply the MK trend with pre-whitening to remove possible autocorrelation of summertime periods (Wang and Swail 2001).

### 4 North America results

We evaluated spatial changes in heat wave patches during the entire record (1950–2013) using simple spatial metrics of individual patch area and the ratio of perimeter to area as well as aggregated metrics of total patch area and patch count. In agreement with previous work by Mazdiyasni and AghaKouchak (2015), we find that the total area of North America that experiences a heat wave has increased through the record (Fig. S1, Table S2). The total number of heat wave patches occurring in each warm season also shows an upward trend through the record (Fig. S2, Table S3). This indicates, as others have found, that both the total area impacted by heat waves and the frequency of these events have increased. We argue that this does not give a complete picture of heat waves; therefore, here, we focus on exploration of the spatial characteristics of individual heat wave patches to further develop an understanding of how heat waves manifest spatially on the surface landscape.

Investigating the empirical cumulative distribution function (CDF) of individual heat wave patch area reveals substantial change in 1982–2013 relative to 1950–1981. The two-sample Kolmogorov-Smirnov (KS) test (see methods) confirms a statistically significant difference between these two periods at the 0.05 significance level for all durations and classes (Table S4). This is further confirmed by an Anderson-Darling test. Figure 1 displays CDFs of individual heat wave patch area for all durations and classes. Heat wave patches have become generally smaller in the latter half of the record with the greatest declines in areal extent occurring in the larger patches (Fig. 1). The leftward shift of the more recent CDF is particularly pronounced in higher classes and longer duration events (Fig. 1).

Similarly to heat wave patch area, we find a substantial change in heat wave patch perimeter/area ratio in 1982–2013 relative to 1950–1981. The KS test again confirms a statistically significant difference between these two periods at the 0.05 significance level



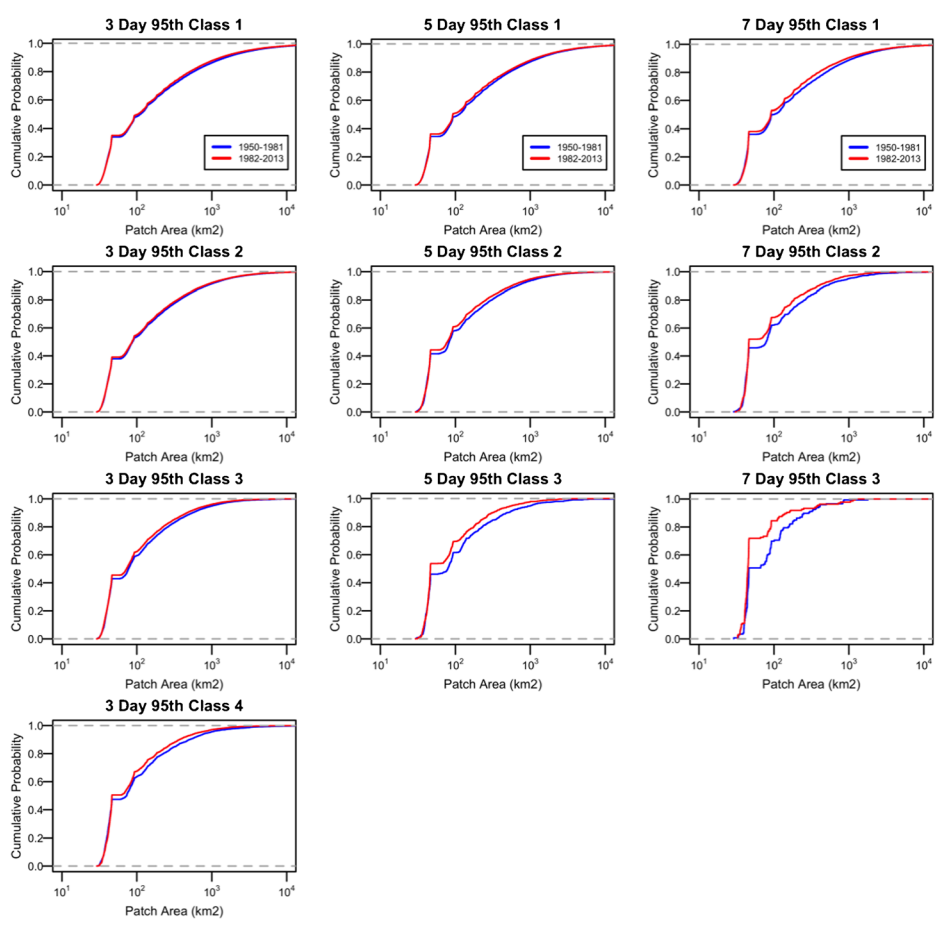


**Fig. 1** The empirical CDF of heat wave patch area from 1950 to 1981 (blue) and 1982–2013 (red) for events above the 95th percentile of daily maximum temperatures. The rows change in heat wave class and the columns change in duration

for all durations and classes (Table S4). Again, this is further confirmed by an Anderson-Darling test. Figure 2 shows the CDFs of individual heat wave patch perimeter/area ratios from 1950 to 1981 and 1982–2013 for all durations and classes. The CDFs from 1982 to 2013 have shifted to the right of those from 1950 to 1981, indicating generally higher perimeter/area ratios in the latter half of the record and, therefore, suggests that heat wave patches have generally become more complex in shape. From this analysis, it also becomes apparent that higher classes and longer duration events have generally higher perimeter/area ratios and exhibit the largest increases in the more recent period.

## 5 Regional results

In order to better determine where changes in spatial characteristics of heat wave patches have occurred within North America, a regional analysis was also performed. Here, the mean values of patch area and perimeter/area ratio of every heat wave patch as well as the total area and count



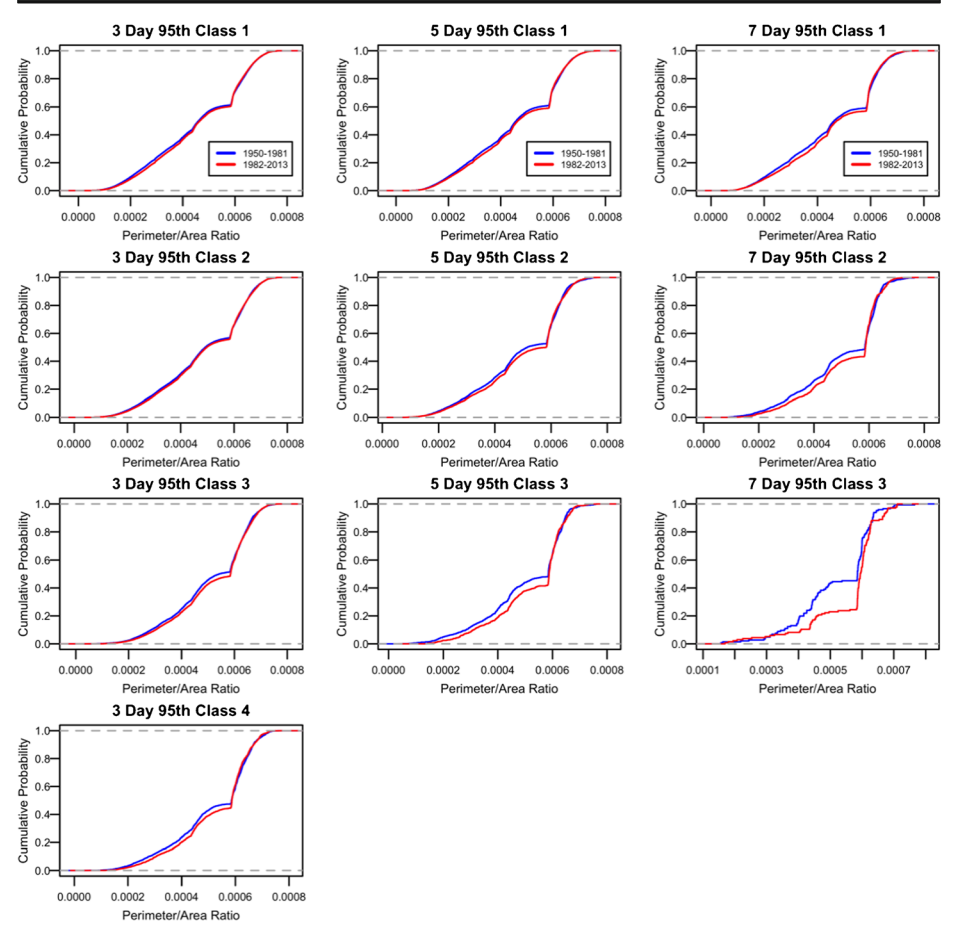


**Fig. 2** The empirical CDF of heat wave patch perimeter/area ratio from 1950 to 1981 (blue) and 1982–2013 (red) for events above the 95th percentile of daily maximum temperature. The rows change in heat wave class and the columns change in duration

of all patches falling within each ecoregion are examined, and the percent difference between 1982 and 2013 and 1950–1981 is calculated. These changes are shown in Figs. 3, 4, and 5. Negative change indicates decreases in the more recent period and positive changes indicate increases in the more recent period. Bar plots show changes between the two time periods for each heat wave class (1–4), and the KS and MK tests are used to highlight regions with statistically significant changes. It is immediately apparent in all figures that mean heat wave patch area has generally decreased by up to 20% or more across the majority of regions (Figs. 3a, 4, and 5a). There is much spatial variability in patch area, but the largest reductions are generally found in the southwest, plains, and southeast. Mean perimeter/area ratio has increased across the majority of regions by up to 10% (Figs. 3b, 4, and 5b). This is particularly apparent in the southwest, plains, southeast, and great lakes. There is a broad trend of increased total patch area across the domain with the largest gains of up to 20% or more found in the southwest, southeast, and Atlantic regions (Figs. 3c, 4, and 5c). Counts of heat wave patches have increased across almost the entire domain with the largest increases in the southwest, southeast, Atlantic, and plains (Figs. 3d, 4, and 5d). In general, there is an apparent pattern across the domain of increases



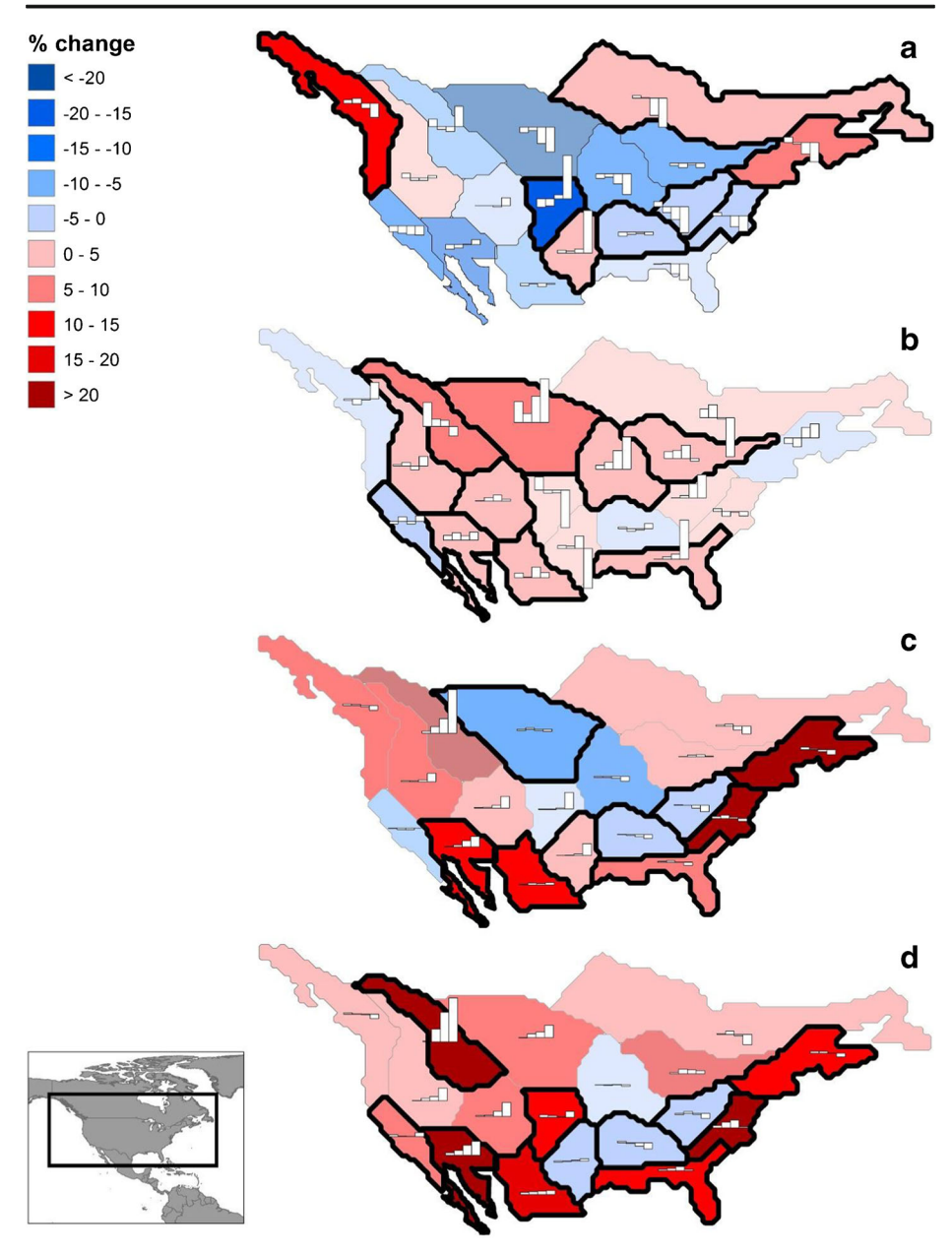
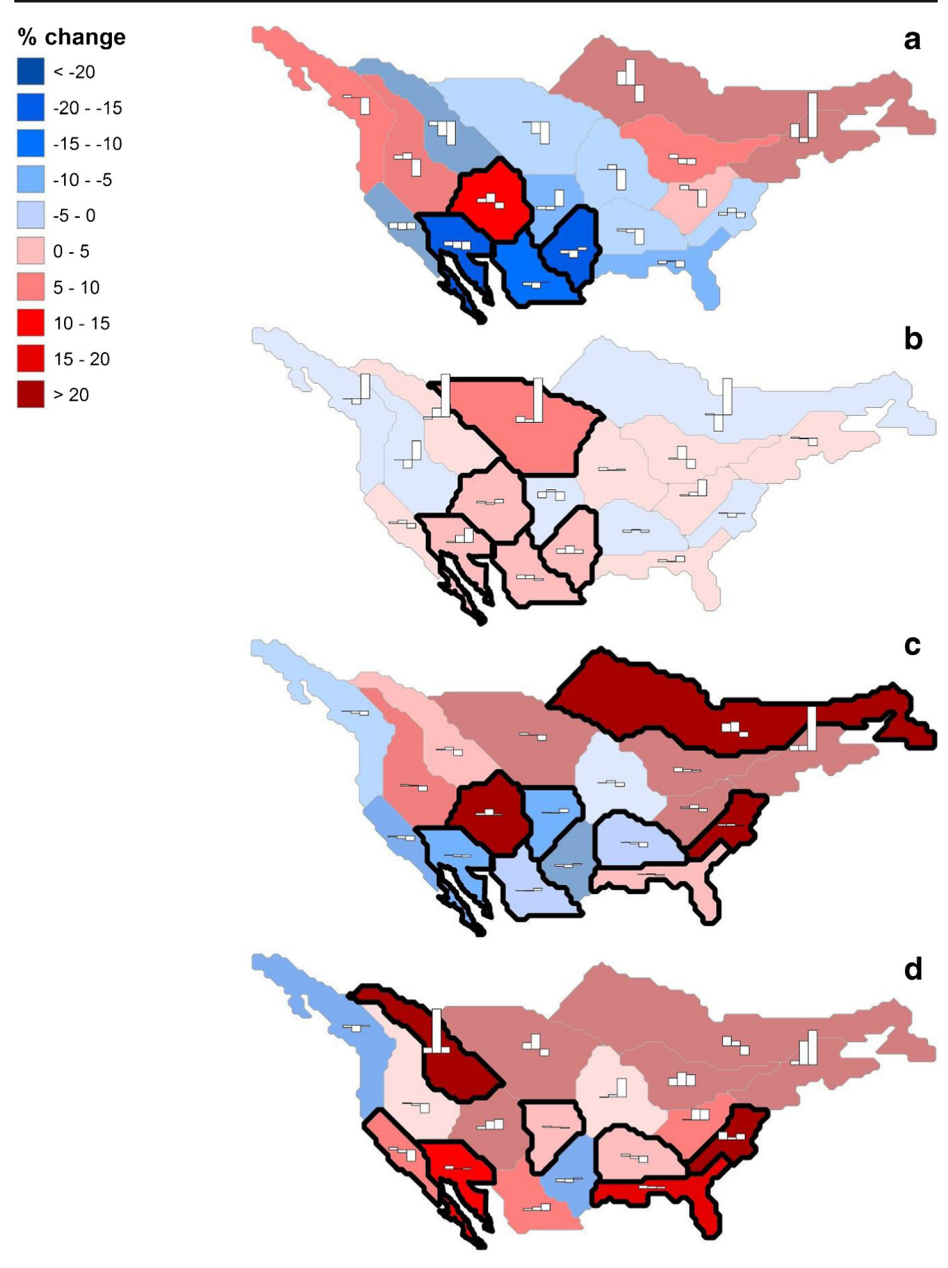


Fig. 3 Change in 3-day events shown as percent difference between 1982–2013 and 1950–1981 by region for the following: a mean heat wave patch area; b mean heat wave patch perimeter/area ratio; c total heat wave patch area; d count of heat wave patches. Positive values indicate increases in the more recent period; negative values indicate decreases in the more recent period. Regions with statistically significant changes, as per the KS/MK test, are outlined in bold black. Non-significant regions are faded. Inset bar plots show percent difference between the two periods by heat wave class for each region

in total heat wave area and count accompanied by decreasing heat wave patch area and increasing heat wave patch shape complexity. Several regions are notable exceptions to this general pattern among the aggregated data. For example, the north Atlantic and northeast Pacific





**Fig. 4** Change in 5-day events shown as percent difference between 1982–2013 and 1950–1981 by region for the following: **a** mean heat wave patch area; **b** mean heat wave patch perimeter/area ratio; **c** total heat wave patch area; **d** count of heat wave patches. Positive values indicate increases in the more recent period; negative values indicate decreases in the more recent period. Regions with statistically significant changes, as per the KS/MK test, are outlined in bold black. Non-significant regions are faded. Inset bar plots show percent difference between the two periods by heat wave class for each region



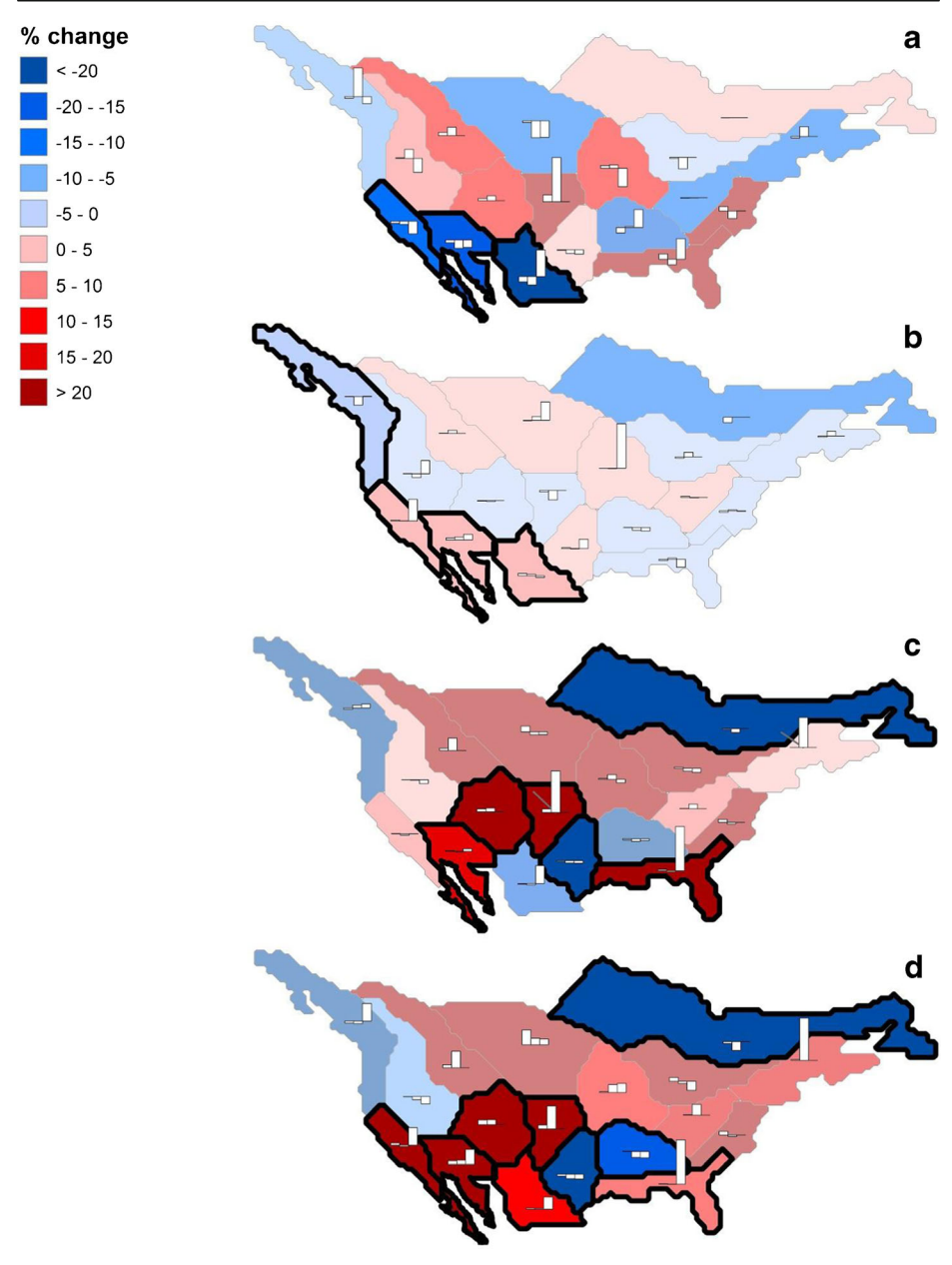


**Fig. 5** Change in 7-day events shown as percent difference between 1982–2013 and 1950–1981 by region for the following: **a** mean heat wave patch area; **b** mean heat wave patch perimeter/area ratio; **c** total heat wave patch area; **d** count of heat wave patches. Positive values indicate increases in the more recent period; negative values indicate decreases in the more recent period. Regions with statistically significant changes, as per the KS/MK test, are outlined in bold black. Non-significant regions are faded. Inset bar plots show percent difference between the two periods by heat wave class for each region



regions exhibit significant increases in 3-day mean patch area, but on closer examination, the higher classes show large reductions in area. It is important to note that across all regions and spatial metrics, the higher classes and longer duration events tend to exhibit the largest changes. These large changes in the more intense classes are not always apparent in the aggregated metrics or significance tests as these classes are by definition more extreme and thus rare.

#### **6 Conclusions**

Past studies have shown that the land area affected by extreme heat has increased through the latter half of the Twentieth Century and that the trend is expected to continue and strengthen during this century (Hansen et al. 2012; Coumou and Robinson 2013; Mazdiyasni and AghaKouchak 2015). The methodology outlined in this paper confirms this upward trend across much of North America while also showing changes in heat waves spatially. The results presented here indicate that, despite an overall increase in the total land area affected by heat and an increase in the frequency of heat waves, there is a reduction in heat wave patch size and increase in the complexity of patch shape. The findings of this paper suggest that heat waves are becoming more fragmented across the land surface of North America. At a regional scale, the southwest, the southeast, and plains exhibit the largest decreases in heat wave patch area and largest increases in shape complexity. It also should be stressed, to avoid misinterpretation of these results, that changes to individual heat wave patches in these areas are accompanied by increases in heat wave total area and frequency, particularly in the higher classes and longer duration events. The conceptual model of heat waves and spatial metrics applied here shows statistical changes in heat waves beyond those that have been hitherto determined through traditional, somewhat aspatial, climatological methods.

A limitation of the current work results from our definition of heat wave patches as single value summertime aggregates of multiple day events, classification of heat waves based on these aggregates, and the subsequent clumping of patches. In this manner, we have simplified and aggregated heat wave patches through each summer. We do lose some of the daily behavior of the patches but still capture the summer season frequency of events in each grid cell and from that we clump adjacent cells with the same summer frequency for analysis as individual patches. The definition of patches in this manner was made essential by considerations of computational expense and, if it were not for the restraints of processing time, the clumping function could certainly be run for each summertime day in every summer allowing for daily fluctuations in grid cells included in a single heat wave patch to be reduced to a core area of 3, 5, or 7 consecutive days of persistent heat. Such an analysis would be conceptually similar to land cover change on a landscape where interiors of a particular patch of a certain land cover are separated into core area versus edge where the edge is more likely to be heterogeneous and in relatively high flux (Mcgarigal 2015). Such a complex analysis is reserved for future work at perhaps a smaller spatial scale of study area.

The spatial configuration (area, fragmentation, shape) of heat waves on the landscape may be of great importance to the understanding of what drives heat wave events and how climate change is interacting with extreme surface temperatures. Heat wave shape may also be a determinant for locating the most intense region within a heat wave patch, just as tropical cyclone shape is an important variable in determining the location of intense precipitation (Matyas 2008; Zick and Matyas 2016). The extent and cohesiveness of heat waves may also be of vital importance to public health planning for emergency management during these



potentially life-threatening events. Further analysis of both large and small-scale atmospheric and land surface drivers of extreme heat are needed to understand the physical processes associated with these spatial changes in heat waves.

**Acknowledgements** This work was funded in part by the Emerging Pathogens Institute at the University of Florida and the College of Liberal Arts and Sciences, as part of the University of Florida Preeminence Initiative.

**Author's contributions** DK conceived the study. DK and EB led data analysis. JE led figure production. DK led in writing and interpretation of the results with assistance from EB and JE.

#### References

- Anderson BG, Bell ML (2009) Weather-related mortality. Epidemiology 20:205–213. https://doi.org/10.1097/EDE.0b013e318190ee08
- Barriopedro D, Fischer EM, Luterbacher J et al (2011) The hot summer of 2010: redrawing the temperature record map of Europe. Science 332(80):220–224. https://doi.org/10.1126/science.1201224
- Bernard SM, Samet JM, Grambsch A et al (2001) The potential impacts of climate variability health effects in the United States. Environ Health Perspect 109:199–209. https://doi.org/10.2307/3435010
- Centers for Disease Control and Prevention (CDC) U (2006) Heat-related deaths—United States, 1999-2003.
  MMWR Morb Mortal Wkly Rep 55:796–798
- Chen Y, Li Y (2017) An inter-comparison of three heat wave types in China during 1961–2010: observed basic features and linear trends. Sci Rep 7:45619. https://doi.org/10.1038/srep45619
- Ciais P, Reichstein M, Viovy N et al (2005) Europe-wide reduction in primary productivity caused by the heat and drought in 2003. Nature 437:529–533. https://doi.org/10.1038/nature03972
- Comrie A (2007) Climate change and human health. Geogr Compass 1:325–339. https://doi.org/10.1111/j.1749-8198.2007.00037.x
- Coumou D, Rahmstorf S (2012) A decade of weather extremes. Nat Clim Chang 2:491–496. https://doi.org/10.1038/nclimate1452
- Coumou D, Robinson A (2013) Historic and future increase in the global land area affected by monthly heat extremes. Environ Res Lett 8:34018. https://doi.org/10.1088/1748-9326/8/3/034018
- Curriero FC, Heiner KS, Samet JM et al (2002) Temperature and mortality in 11 cities of the eastern United States. Am J Epidemiol 155:80–87. https://doi.org/10.1093/aje/155.1.80
- DeGaetano AT, Allen RJ (2002) Trends in twentieth-century temperature extremes across the United States. J Clim 15:3188–3205. https://doi.org/10.1175/1520-0442(2002)015<3188:TITCTE>2.0.CO;2
- Diffenbaugh NS, Ashfaq M (2010) Intensification of hot extremes in the United States. Geophys Res Lett. https://doi.org/10.1029/2010GL043888
- Easterling DR, Meehl GA, Parmesan C et al (2000) Climate extremes: observations, modeling, and impacts. Science 289:2068–2074. https://doi.org/10.1126/science.289.5487.2068
- Ebi KL (2008) Using health models to prepare for and cope with climate change. Clim Change 88(1):1-3
- Gaffen DJ, Ross RJ (1998) Increased summertime heat stress in the US. Nature 396:529–530. https://doi. org/10.1038/25030
- Grose MR, Risbey JS, Whetton PH (2017) Tracking regional temperature projections from the early 1990s in light of variations in regional warming, including "warming holes". Clim Chang 140:307–322. https://doi.org/10.1007/s10584-016-1840-9
- Hajat S, Kovats RS, Atkinson RW, Haines A (2002) Impact of hot temperatures on death in London: a time series approach. J Epidemiol Community Health 56:367–372. https://doi.org/10.1136/jech.56.5.367
- Hajat S, Armstrong B, Baccini M et al (2006) Impact of high temperatures on mortality: is there an added heat wave effect? Epidemiology 17:632–638. https://doi.org/10.1097/01.ede.0000239688.70829.63
- Hansen J, Sato M, Ruedy R (2012) Perception of climate change. Proc Natl Acad Sci U S A 109:E2415–E2423. https://doi.org/10.1073/pnas.1205276109
- Hattis D, Ogneva-Himmelberger Y, Ratick S (2012) The spatial variability of heat-related mortality in Massachusetts. Appl Geogr 33:45–52. https://doi.org/10.1016/j.apgeog.2011.07.008
- IPCC (2014) Climate change 2014: synthesis report. Contribution of working groups I, II and III to the fifth assessment report of the intergovernmental panel on climate change. IPCC, Geneva
- Keellings D, Waylen P (2014a) Increased risk of heat waves in Florida: characterizing changes in bivariate heat wave risk using extreme value analysis. Appl Geogr 46:90–97. https://doi.org/10.1016/j.apgeog.2013.11.008



- Keellings D, Waylen P (2014b) Investigating teleconnection drivers of bivariate heat waves in Florida using extreme value analysis. Clim Dyn 44:3383–3391. https://doi.org/10.1007/s00382-014-2345-8
- Kendall MG (1955) Rank correlation methods. Charles Griffin, London
- Kumar S, Kinter J, Dirmeyer PA et al (2013) Multidecadal climate variability and the "warming hole" in north america: results from CMIP5 twentieth- and twenty-first-century climate simulations. J Clim 26:3511–3527. https://doi.org/10.1175/JCLI-D-12-00535.1
- Kunkel KE, Liang X-Z, Zhu J, Lin Y (2006) Can CGCMs simulate the twentieth-century "warming hole" in the central United States? J Clim 19:4137–4153. https://doi.org/10.1175/JCLI3848.1
- Kunst AE, Looman CW, Mackenbach JP (1993) Outdoor air temperature and mortality in The Netherlands: a time-series analysis. Am J Epidemiol 137:331–341
- Leibensperger EM, Mickley LJ, Jacob DJ et al (2012) Climatic effects of 1950-2050 changes in US anthropogenic aerosols-part 2: climate response. Atmos Chem Phys 12:3349–3362. https://doi.org/10.5194/acp-12-3349-2012
- Livneh B, Bohn TJ, Pierce DW et al (2015) A spatially comprehensive, hydrometeorological data set for Mexico, the U.S., and southern Canada 1950-2013. Sci data 2:150042. https://doi.org/10.1038/sdata.2015.42
- Mann HB (1945) Nonparametric tests against trend. Mann Source Econom 13:245–259. https://doi. org/10.1017/CBO9781107415324.004
- Matyas C (2008) Shape measures of rain shields as indicators of changing environmental conditions in a landfalling tropical storm. Meteorol Appl 15:259–271. https://doi.org/10.1002/met.70
- Maurer EP, Wood AW, Adam JC et al (2002) A long-term hydrologically based dataset of land surface fluxes and states for the conterminous United States\*. J Clim 15:3237–3251. https://doi.org/10.1175/1520-0442(2002)015 <3237:ALTHBD>2.0.CO;2
- Mazdiyasni O, AghaKouchak A (2015) Substantial increase in concurrent droughts and heatwaves in the United States. Proc Natl Acad Sci 112:11484–11489. https://doi.org/10.1073/pnas.1422945112
- McGarigal K (2015) Fragstats help 2015. Available online: http://www.umass.edu/landeco/research/fragstats/documents/fragstats.help.4.2.pdf
- Mearns LO, Arritt R, Biner S et al (2012) The north American regional climate change assessment program. Bull Am Meteorol Soc 93:1337–1362. https://doi.org/10.1175/BAMS-D-II-00223.1
- Meehl GA, Tebaldi C (2004) More intense, more frequent, and longer lasting heat waves in the 21st century. Science 305(80-):994–997. https://doi.org/10.1126/science.1098704
- Meehl GA, Arblaster JM, Branstator G (2012) Mechanisms contributing to the warming hole and the consequent U.S. east-west differential of heat extremes. J Clim 25:6394–6408. https://doi.org/10.1175/JCLI-D-11-00655.1
- Meehl GA, Arblaster JM, Chung CTY (2015) Disappearance of the southeast U.S. "warming hole" with the late 1990s transition of the Interdecadal Pacific oscillation. Geophys Res Lett 42:5564–5570. https://doi. org/10.1002/2015GL064586
- Mora C, Dousset B, Caldwell IR et al (2017) Global risk of deadly heat. Nat Clim Chang 7:501–506. https://doi.org/10.1038/nclimate3322
- Pan Z, Liu X, Kumar S et al (2013) Intermodel variability and mechanism attribution of central and southeastern U.S. anomalous cooling in the twentieth century as simulated by CMIP5 models. J Clim 26:6215–6237. https://doi.org/10.1175/JCLI-D-12-00559.1
- Peng RD, Bobb JF, Tebaldi C, McDaniel L, Bell ML, Dominici F (2011). Toward a quantitative estimate of future heat wave mortality under global climate change. Environ Health Perspect 119(5):701
- Perkins SE, Pitman AJ, Sisson SA (2013) Systematic differences in future 20 year temperature extremes in AR4 model projections over Australia as a function of model skill. Int J Climatol 33:1153–1167. https://doi.org/10.1002/joc.3500
- Photiadou C, Jones MR, Keellings D, Dewes CF, (2014) Modeling european hot spells using extreme value analysis. Clim Res 58(3):193–207
- Robinson WA, Reudy R, Hansen JE (2002) General circulation model simulations of recent cooling in the east-central United States. J Geophys Res Atmos. https://doi.org/10.1029/2001JD001577
- Schlenker W, Roberts MJ (2009) Nonlinear temperature effects indicate severe damages to U.S. crop yields under climate change. Proc Natl Acad Sci 106:15594–15598. https://doi.org/10.1073/pnas.0906865106
- Sekhon JS (2011) Multivariate and propensity score matching software with automated balance optimization: the matching package for R. J Stat Softw 42(7):1–52.
- Shepard DS (1984) Computer mapping: The SYMAP interpolation algorithm. In: Gaile GL and Willmott CJ (eds) Spatial statistics and models. Springer, Dordrecht, pp. 133–145.
- Stephens MA (1970) Use of the Kolmogorov-Smirnov, Cramer-von Mises and related statistics without extensive tables. J R Stat Soc Ser B 32:115–122. https://doi.org/10.1038/203024b0
- Tan J, Zheng Y, Song G, Kalkstein L, Kalkstein A, Tang X (2007) Heat wave impacts on mortality in Shanghai, 1998 and 2003. Int J Biometeorol 51(3):193–200



- Toomey M, Roberts DA, Still C et al (2011) Remotely sensed heat anomalies linked with Amazonian forest biomass declines. Geophys Res Lett. https://doi.org/10.1029/2011GL049041
- Vautard R, Honore C, Beekmann M, Rouil L (2005) Simulation of ozone during the august 2003 heat wave and emission control scenarios. Atmos Environ 39:2957–2967
- Wang H, Schubert S, Suarez M et al (2009) Attribution of the seasonality and Regionality in climate trends over the United States during 1950–2000. J Clim 22:2571–2590. https://doi.org/10.1175/2008JCLI2359.1
- Wang XL, Swail VR (2001) Changes of extreme Wave Heights in northern hemisphere oceans and related atmospheric circulation regimes. J Clim 14:2204–2221. https://doi.org/10.1175/1520-0442(2001)014<2204:COEWHI>2.0. CO:2
- Widmann M, Bretherton CS (2000) Validation of mesoscale precipitation in the NCEP reanalysis using a new gridcell dataset for the northwestern United States. J Clim 13:1936–1950. https://doi.org/10.1175/1520-0442 (2000)013<1936:VOMPIT>2.0.CO:2
- Yu S, Alapaty K, Mathur R et al (2014) Attribution of the United States "warming hole": aerosol indirect effect and precipitable water vapor. Sci Rep 4:6929. https://doi.org/10.1038/srep06929
- Zaitchik B, Macalady AK, Bonneau LR, Smith RB (2006) Europe's 2003 heatwave: a satellite view of impacts and land-atmosphere feedbacks. Int J Climatol 26:743–769
- Zamuda C, Mignone B, Bilello D, Hallett KC, Lee C, Macknick J, Newmark R, Steinberg D (2013) US energy sector vulnerabilities to climate change and extreme weather (No. DOE/PI-0013). Department of Energy, Washington DC
- Zick SE, Matyas CJ (2016) A shape metric methodology for studying the evolving geometries of synoptic-scale precipitation patterns in tropical cyclones. Ann Am Assoc Geogr 106:1217–1235. https://doi.org/10.1080/24694452.2016.1206460

